*Desalination and Water Treatment*
www.deswater.com

doi: 10.5004/dwt.2020.25757

192 (2020) 371–381
July

# Effects of various factors on photodegradation-induced changes in spectroscopic characteristics and chlorine reactivity of transphilic acid in ice

Shuang Xue*, Siyu Zhao, Xuefeng Guan, Chao Wang, Zhonglin Chen*, Qiang Liu

*School of Environmental Science, Liaoning University, Shenyang 110036, China, Fax: +86-2462204818;*
*emails: xueshuang666@sina.com (S. Xue), 15524435643m@sina.com (Z.L. Chen), 1493504491@qq.com (S.Y. Zhao), 125442597@qq.com (X.F. Guan), wangchao9900@126.com (C. Wang), Liuqiang_lnu@sina.com (Q. Liu)*

Received 14 July 2019; Accepted 28 February 2020

**ABSTRACT**

This study investigated the photodegradation of transphilic acid (TPI-A) in ice under natural solar radiation, as well as the effect of various environmental factors, such as pH, salinity, the concentrations of iron (Fe), nitrate ($NO_3^-$), and original dissolved organic carbon (DOC) concentration, on the content, spectroscopic characteristics and chlorine reactivity of TPI-A in ice in the photodegradation process. TPI-A was isolated using XAD resins from water samples collected from the Hunhe River in Liaoning Province, China. The results showed, that in the photodegradation process of TPI-A in the ice, compared with neutral conditions, both acidic and alkaline conditions accelerated DOC and ultraviolet (UV) absorbance at 254 nm (UV-254) removal rates. High pH conditions effectively accelerated the photodegradation of fluorescent materials and trihalomethane (THM) precursors in TPI-A. The salinity inhibited the photodegradation of UV-absorbing compounds, THM precursors, and aromatic protein-like, fulvic acid-like, and soluble microbial byproduct-like (SMP-like) fluorescent materials in TPI-A. The influences of Fe concentration over the photodegradation of TPI-A and total fluorescent materials in it were small. $NO_3^-$ accelerated the photodegradation of TPI-A while it had an inhibition effect over five types of fluorescent materials in TPI-A. The lower the initial DOC concentration was, the higher the photodegradation rates TPI-A and THM precursors in it.

*Keywords:* Transphilic acid; Photodegradation; Ice; Influencing factors

## 1. Introduction

Dissolved organic matter (DOM) is a complex mixture of organic compounds, which is known to plays an important role in the fate and transport of many toxic organic or inorganic chemicals and nutrient cycling throughout the environment [1,2]. DOM acts also as the most important precursor of disinfection by-products and enables the microorganisms to grow in the treatment unit or distribution system [3]. No single analytical tool, however, can provide definitive structural or functional information about DOM because of its heterogeneous, ill-defined nature [2]. Fractionation of total natural organic matters (NOM) offers advantages by selectively separating one group of organic compounds (or a subcomponent) from the others based on their physical and chemical properties [2,4]. XAD resin method has been reported in many applications for fractionation of DOM and is generally considered as the state-of-art method at present for such fractionation [3]. Among DOM fractions isolated by XAD resins, hydrophobic acid (HPO-A) has been the focus of several studies in the past decades assessing the characteristics and behavior of DOM [4]. Yet, transphilic acid (TPI-A), which is generally the second-most abundant DOM fraction in natural waters and exhibits high chlorine reactivity has so far received much less attention

* Corresponding authors.

[5]. The DOM fractions are operationally defined. TPI-A is those compounds that adsorb onto XAD-4 resin and are dissolved during back elution with NaOH [6]. The content of TPI-A in surface waters is generally lower than HPI-A, but higher than the other DOM fractions, such as hydrophobic neutral (HPO-N), transphilic neutral (TPI-N), and a hydrophilic fraction (HPI). Carbon-13 nuclear magnetic resonance spectroscopy ($^{13}$C-NMR) spectra of TPI-A showed more oxygenated aliphatic groups and carboxyl groups than HPO-A. Aiken et al. [7] reported that TPI-A was lower in molecular weight with greater heteroatom and carboxyl content than HPO-A. The chlorine reactivity of TPI-A with chlorine in producing trihalomethanes (THMs) is generally lower than that of HPO-A but is higher than HPO-N, TPI-N, and HPI [8,9]. Proton nuclear magnetic resonance spectroscopy ($^{1}$H-NMR) analysis showed that the relative contents of aliphatic protons in TPI-A were higher than other fractions [8]. TPI-A has higher molar values of oxygen to carbon and nitrogen to carbon ratios [8]. Fourier-transform infrared spectra of TPI-A showed that carboxylic acids existed as a major functional group in TPI-A, and aliphatic C–H and the amide-2 functional group were also present in TPI-A [10].

DOM was one of the most important light absorption components which were likely to be conversed by the photochemical process [11–13]. In recent decades, the researchers have become more and more aware of the significance of the photochemical conversion process of DOM to the global carbon cycle, its biogeochemistry behaviors, and ecological environmental effect [14–16]. Due to the poor biodegradability of TPI-A [5], photodegradation played a significant role in the characteristics and geochemical behavior of TPI-A.

Surface waters in regions of middle and high latitudes are usually ice-covered for several months. In the freezing process of water, pollutants would inevitably enter the ice layer. As a non-liquid medium, the physical transport process, conventional chemical reactions, and microbial degradation of the pollutants in the ice layer were relatively weak, however, the photochemical action plays a critical role in the contents as well properties of pollutants in ice [17,18]. Thus, it is essential to investigate the photodegradation of the pollutants in the ice for a better understanding of the distribution, migration, and transformation of pollutants in the water environment in the frozen period. It was reported that environmental conditions, such as pH, salinity, and concentrations of inorganic ions, are important factors affecting the photodegradation of pollutants in water [11,19–21].

Our previous studies have investigated the photodegradation of bulk DOM with different origins in ice as well as the impact of some environmental factors on the changes in dissolved organic carbon (DOC) concentrations of DOM in ice induced by photodegradation [22]. However, the effects of environmental factors on photodegradation-induced changes in spectroscopic characteristics and chlorine reactivity of bulk DOM and individual DOM fractions in ice are still unclear. Thus, the main purpose of this study was to examine the effect of various environmental factors, such as pH, salinity, the concentrations of iron (Fe), nitrate ($NO_3^-$), and DOC concentration on the content, spectroscopic characteristics and chlorine reactivity of TPI-A in ice in the photodegradation process.

## 2. Material and methods

### 2.1. Sample collection and preservation

Water samples for this study were collected from the Hunhe River on 27 November 2013. Hunhe River is a major river in Shenyang, Liaoning Province. Water samples were carefully collected and transferred to the laboratory in an ice cooler and stored at 4°C to minimize changes in the constituents. The characteristics of the Hunhe River water samples were summarized in Table 1.

### 2.2. Isolation of TPI-A

Water samples were filtered using a 0.45 μm cellulose nitrate membrane filter. Then, 0.45 μm filtrates were acidified to pH 2 and passed through two columns in series containing XAD-8 and XAD-4 resins. After all the samples were run through the columns, each column was separately back eluted with 0.1 mol/L NaOH. The eluate from XAD-8 is defined as HPO-A and the eluate from XAD-4 is defined as TPI-A [23]. HPO-N and TPI-N are those compounds that adsorb onto XAD-8 and XAD-4 resins, respectively, but are not dissolved during back elution with NaOH. They were desorbed from the XAD resins using a 75% acetonitrile/25% Milli-Q water solution (Milli-pore Company, America). Acetonitrile was subsequently removed using

Table 1
Characteristics of Hunhe River water samples

| Parameter | Value | Parameter | Value |
|---|---|---|---|
| pH | 6.8 | UV-254 ($m^{-1}$) | 7.7 |
| Total organic carbon (mg $L^{-1}$) | 6.2 | Turbidity (NTU) | 5.9 |
| Dissolved organic carbon (mg $L^{-1}$) | 5.1 | Conductivity (ms $cm^{-1}$) | 323.6 |
| Alkalinity (mg $L^{-1}$) | 7.2 | Sulfate (mg $L^{-1}$) | 63.31 |
| Hardness (mg $L^{-1}$) | 132 | Bromide (mg $L^{-1}$) | Nd[a] |
| Fe (mg $L^{-1}$) | 0.14 | Chloride (ug $L^{-1}$) | 0.17 |
| Mn (mg $L^{-1}$) | 0.021 | Cu (mg $L^{-1}$) | 0.001 |
| Cd (mg $L^{-1}$) | 0.010 | Zn (mg $L^{-1}$) | 0.006 |

[a]below the detection limit of 20 mg/L.

rotary-evaporation and the resin isolates were lyophilized. HPI is the carbon in the XAD-4 effluent. The DOM fractionation results showed that HPO-A, HPO-N, TPI-A, TPI-N, and HPI accounted for 39%, 9%, 29%, 7%, and 16% of DOC in the Hunhe River water samples, respectively. The isolated TPI-A samples were adjusted to pH 7 and then desalted using cation exchange resin.

### 2.3. Effects of various factors on TPI-A photodegradation experiments

Natural water bodies have different water chemical components, such as different pH values (5 to 9) [24] and different concentrations of $Fe^{3+}$ (1.2 to 16.8 umol/L) [25], $NO^{3-}$ ($10^{-5}$ to $10^{-3}$ mol/L) [26], which directly or indirectly affect the photodegradation of DOM [27]. In estuarine areas, pH values have been increasing during the mixing process from freshwater to seawater, the ionic strength and salinity (0 to 34.6) also increase from river water to seawater [28,29]. To evaluate the effect of pH on the photodegradation of TPI-A, 6 mol $L^{-1}$ NaOH solution and 6 mol $L^{-1}$ HCl solution were used to adjust the pH to 3.0, 5.0, 7.0, 9.0, and 13.0, respectively. The co-existing ions on TPI-A photodegradation in ice including Fe (0 to 5.6 mg/L) and $NO_3^-$ (0 to 0.5 mg/L) were adjusted by the addition of ferric chloride ($FeCl_3$) and sodium nitrate ($NaNO_3$), respectively. The water samples were dosed with seawater salt to adjust them to different salinities (0 to 30). The TPI-A water sample with a DOC of 8.5 mg $L^{-1}$ which were diluted with ultra-pure water (Milli-Q) into 8.5–2.8 mg $L^{-1}$. In addition, the photodegradation experiments were also conducted on black samples, which were wrapped with aluminum foil to prevent transformation by sunlight in the photodegradation experiments. The water samples were put into the quartz colorimetric tubes (inner diameter × height × wall thickness = 28 mm × 380 mm × 2 mm) respectively, then, they were placed in the refrigerator for 2 h to freeze. The weather was clear within the experiment period with a solar radiation period of 8:00–16:00 each day. The samples were replaced into the refrigerator during another period. The temperature during the solar radiation period was –18°C ~ –27°C. The total solar radiation period was 20 d (total 160 h), with the intensity of solar radiation ranging from 579 to 980 lux. After photodegradation experiments, all samples were got back and melted at room temperature.

### 2.4. Analysis

DOC was analyzed using a Shimadzu TOC-5000 (Japan) total organic carbon analyzer with auto-sampler. Ultraviolet (UV) absorbance at 254 nm (UV-254) was measured with a Cary 50 ultraviolet-visible (UV/VIS) spectrophotometer (Varin Company, America) at 254 nm using a quartz cell with a 1 cm path-length. The instrument was zeroed using Milli-Q water as a blank. Specific ultraviolet light absorbance (SUVA) was calculated as (UV-254/DOC) × 100. Bromide ion concentrations were determined using an Agilent ZORBAX ion chromatographic (IC) system (Sunnyvale, CA, America).

Trihalomethane formation potential (THMFP) measurements were performed according to Standard Method 5710B. The chlorine dosage for each water sample was determined such that the final residual chlorine of 3–5 mg $L^{-1}$ remained in the sample after the 7 d of incubation at 25°C. All samples were adjusted to a pH of 7 ± 0.2 using $H_2SO_4$ and NaOH. The neutralized solution was then buffered with a phosphate solution prior to incubation in amber bottles at 25°C ± 2°C for 7 d. At the end of the incubation period, samples were dechlorinated using sodium sulfite ($Na_2SO_3$). THMs were extracted with methyl tert-butyl ether from the chlorinated samples using a modified Environment Protection Agency Method 551.1 and analyzed by gas chromatography (CP-3800) with an electron capture detector. For all THMFP measurements in this study, only chloroform ($CHCl_3$) was measured and bromodichloromethane ($CHCl_2Br$), dibromochloromethane ($CHClBr_2$) and bromoform ($CHBr_3$) were not detected. The absence of the bromine-containing THMs ($CHCl_2Br + CHBr_2Cl + CHBr_3$) in the THMFP measurements was expected since $Br^-$ in the Hunhe River water samples was lower than the detection limit of 20 mg/L. Therefore, THMFP was, in fact, $CHCl_3$ formation potential in this study.

Fluorescence spectra were obtained with a JASCO FP-6500 spectrofluorometer (Varin Company, America). The spectrofluorometer used a Xenon excitation source, and the slits set to 5 nm for both excitation and emission. Filtered water extracts were diluted to 1 mg $L^{-1}$ of DOC with 0.01 mol $L^{-1}$ KCl. The emission (Em) wavelength range was fixed from 290 to 550 nm (1 nm intervals), whereas the excitation (Ex) wavelength was increased from 220 to 400 nm (5 nm intervals). Scan speed was set at 1,000 nm $min^{-1}$, generating an excitation-emission matrix (EEM) in about 15 min. Blank sample (0.01 mol $L^{-1}$ KCl) fluorescence was subtracted from all spectra. To eliminate the Rayleigh scattering interference in EEMs, the intensity values at points where the emission wavelength was the same as or twice the excitation wavelength, as well as those adjacent to them (±10 nm emission wavelength at the same excitation wavelength), were excised from the scan data and the excised values were replaced with zero [30]. In addition, this procedure was also applied to the data points in EEMs with an emission wavelength < the excitation wavelength or >twice the excitation wavelength. All data points whose value had been replaced with zero were excluded when calculating projected excitation-emission area in quantitative analyses of EEM spectra by means of the fluorescence regional integration (FRI) technique proposed by Chen et al. [5].

## 3. Results and discussion

### 3.1. Dissolved organic carbon

The DOC values of all samples in the photodegradation experiment are shown in Fig. 1. Before illumination, each environmental factor had little influence on DOC, and after 3 h of illumination, DOC content significantly decreased under each condition. With the increase of pH, DOC removal rate increases first and then decreases. Under alkaline conditions, the removal rate of DOC was higher than that under neutral and acidic conditions. With the increase of salinity, the removal rate of DOC in water samples increased first and then decreased (Fig. 1b). When the salinity is 5, the highest removal rate of DOC is 86.8%. The results of this study are different from those of Cottrell et al. [11]. However, Cottrell et al. [11] found that there was no significant correlation between the photodegradation

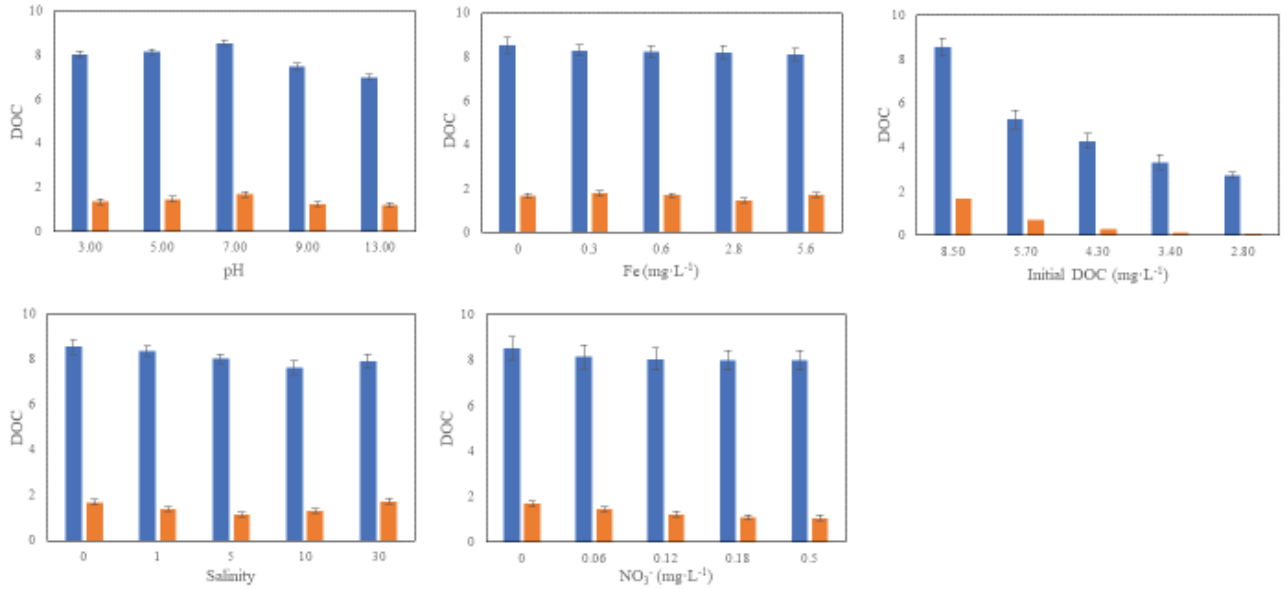


Fig. 1. DOC for samples (a) with different pH, (b) with different Fe concentrations, (c) with different salinity values, (d) with different $NO_3^-$ concentrations, and (e) with different initial DOC values before and after photolysis 3 h.

rate of DOM in wastewater and salinity. The differences in the observed results may be attributed to the different DOM types (DOM fraction isolated by XAD resins vs. bulk DOM) and the different media (ice vs. water); Fe concentration had weak effects on DOC photodegradation rate and the effects were lack of regularity (Fig. 1c). As can be seen from Fig. 1d, increasing the concentration of $NO_3^-$ can accelerate the photodegradation of DOC, but the overall change is not great. When the initial DOC is 8.5, 5.7, 4.3, 3.4, and 2.8 mg $L^{-1}$, the DOC removal rates are 80.2%, 87.5%, 93.2%, 96.5%, and 96.5% respectively (Fig. 1e). The results showed that the lower the initial DOC concentration, the better the photodegradation of DOC. This phenomenon may be quantified by the solar energy injected into the sample, and TPI-A is a surplus for this energy. When the same amount of solar energy is absorbed by a small amount of TPI-A, the degradation efficiency is obviously improved, and the removal rate of DOC is also higher.

The maximum differences in DOC removal rates were caused by variations of pH, salinity, Fe concentration, $NO_3^-$ concentration, and original DOC concentration were 6.0%, 7.0%, 3.8%, 7.4% and 16.3%, respectively. The results suggested that these factors had weak effects on the photodegradation of TPI-A in ice and the influence abilities ranking was as follows: initial DOC concentration > $NO_3^-$ concentration > salinity > pH > Fe concentration.

### 3.2. UV-254 and SUVA

UV-254 is mainly caused by electron-rich sites, such as aromatic functional groups and double-bonded C groups in the DOM molecule. SUVA is calculated by UV-254 divided by the DOC of the water sample. Therefore, UV-254 and SUVA have frequently been used as an indicator of the aromaticity of NOM and its reactivity with oxidants such as chlorine ($Cl_2$) and ozone ($O_3$) [31].

The UV-254 values of all samples after 120 h solar radiation were shown in Fig. 2. The UV-254 removal rates of samples with pH = 3.0, 5.0, 7.0, 9.0, and 11.0 were 94.6%, 93.1%, 91.1%, 94.8%, and 97.2%, respectively, which suggested that, as compared with neutral condition, increasing the acidity/alkalinity of the medium were a benefit for removal of the unsaturated chemical structure of C=C, C=O and benzene ring, etc. contained in the samples by photodegradation. The UV-254 of samples with salinities of 0, 1, 5, and 10, 30 reduced by 91.1%, 91.4%, 90.3%, 83.2%, and 75.3%, respectively. Thus, it could be seen that high salinity inhibited the UV-254 reduction, in the photodegradation process of TPI-A in ice. When Fe concentrations were at 0, 0.3, 0.6, 2.8, and 5.6 mg $L^{-1}$, the UV-254 removal rates of samples were 91.1%, 91.3%, 93.3%, 93.1%, and 90.0%, respectively. Thus, it could be concluded from the results that when Fe concentration was lower than 0.6 mg $L^{-1}$, the increases of Fe concentration accelerated UV-254 removal; but when Fe concentration was higher than 0.6 mg $L^{-1}$, further increases of $FeCl_3$ concentration inhibited UV-254 removal. In this study, the best Fe concentration for UV-254 removal was 0.6 mg $L^{-1}$. When $NO_3^-$ concentrations were 0, 0.06, 0.12, 0.18, and 0.50 mg $L^{-1}$, the UV-254 removal rate of samples was 91.1%, 96.0%, 88.2%, 90.0%, and 93.8%, respectively. The best $KNO_3$ concentration for UV-254 removal was 0.06 mg $L^{-1}$. The corresponding UV-254 values of samples with the initial DOC concentration of 8.5, 5.7, 4.3, 3.4, and 2.8 mg $L^{-1}$ were respectively: 0.18, 0.12, 0.09, 0.07, and 0.06 $cm^{-1}$ before solar irradiation and 16 × $10^{-3}$, 13 × $10^{-3}$, 8 × $10^{-3}$, 6 × $10^{-3}$, 6 × $10^{-3}$ $cm^{-1}$ after solar irradiation. Even though the UV-254 value of samples decreased with the decrease of initial DOC concentration, the removal rates fluctuated within the range of 90.8% ± 1.5%, indicating that the initial DOC concentration has less influence on UV-254 removal rates.

The SUVA value for the original TPI samples which were not subjected to the photodegradation experiments

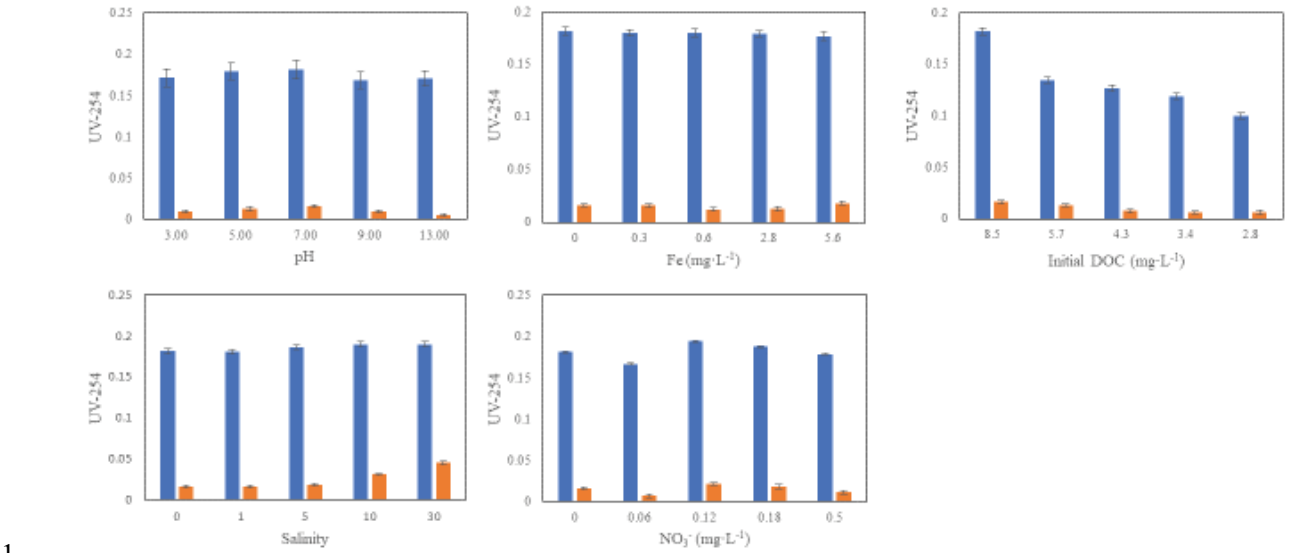


Fig. 2. UV-254 for samples (a) with different pH, (b) with different Fe concentrations, (c) with different salinity values, (d) with different $NO_3^-$ concentrations, and (e) with different initial DOC values before and after photolysis 3 h.

was 2.13 L $mg^{-1}$ $m^{-1}$. This value was consistent with SUVA values of DOM fractions reported in literature where HPO-A, HPO-N, TPI-A, TPI-N, and HPI exhibited SUVA values of 2.0–3.6 L $mg^{-1}$ $m^{-1}$, 1.5–3.8 L $mg^{-1}$ $m^{-1}$, 1.5–3.0 L $mg^{-1}$ $m^{-1}$, 1.5–1.8 L $mg^{-1}$ $m^{-1}$, and 0.9–1.7 L $mg^{-1}$ $m^{-1}$ [8,28,31,32]. On the other hand, the SUVA values of TPI-A in irradiated samples ranged from 0.43 to 5.78 L $mg^{-1}$ $m^{-1}$, and the changes in SUVA was caused by photodegradation.

As shown in Fig. 3, solar irradiation decreased the SUVA of the samples by 54.9%, which suggested that the removal rate of UV-absorbing compounds resulted from photodegradation was higher than that of the bulk organics represented by DOC. The maximum differences in SUVA changes caused by variations of pH, salinity, Fe concentration, $NO_3^-$ concentration, and original DOC concentration were 24.8%, 77.0%, 16.5%, 59.1%, and 226.2%, respectively. Thus, it could be seen that in the photodegradation process of TPI-A in ice, initial DOC concentration had a great influence on SUVA.

The SUVA decrease rate of samples with pH = 3.0, 5.0, 7.0, 9.0, and 11.0 were 65.7%, 59.6%, 54.9%, 63.9%, and 79.8%, respectively. The results suggested that both increases of pH (pH > 7.0) and decreases of pH (pH < 7.0) resulted in higher removal rates of UV-absorbing compounds than the bulk organics represented by DOC, in the photodegradation process of TPI-A in ice. With increases of

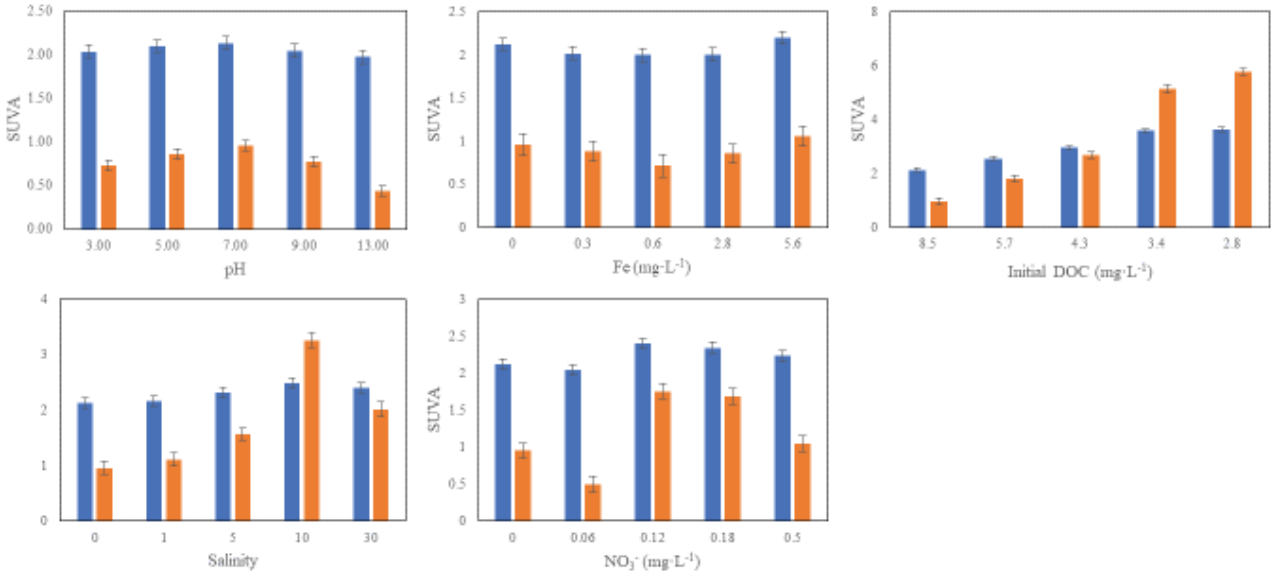


Fig. 3. SUVA for samples (a) with different pH, (b) with different Fe concentrations, (c) with different salinity values, (d) with different $NO_3^-$ concentrations, and (e) with different initial DOC values before and after photolysis 3 h.

salinity, the SUVA decrease rate decreased from –22.1% to 54.9%, indicating that high salinity inhibited the decrease in aromaticity of TPI-A, in the photodegradation process of TPI-A in ice. When salinity was 10, the inhibition reached its peak. With increases of Fe concentration, SUVA in TPI-A increased initially and then decreased. The lowest SUVA value was observed in the sample with a Fe concentration of 0.6 mg $L^{-1}$. The influence of $NO_3^-$ concentration on SUVA was lack of regularity. In this study, the best $NO_3^-$ concentration for SUVA reduction was 0.06 mg $L^{-1}$. With the decreases in initial DOC concentration, SUVA decrease rate of samples decreased from –171.4% to 54.9%, thus, it could be seen that increases of initial DOC concentration resulted in a higher photodegradation rate of UV-absorbing compounds as compared with the bulk organics represented by DOC.

### 3.3. Fluorescence spectra

To analyze quantitatively EEM spectra, EEM spectra were divided into five regions using consistent excitation and emission wavelength boundaries (Fig. 4). The five regions were as follows: regions I (Ex: 220–250 nm–Em: 290–330 nm) and II (Ex: 220–250 nm–Em: 330–380 nm) recognized as belonging to aromatic protein-like fluorescence, region III (Ex: 220–250 nm–Em: 380–550 nm) associated with fulvic acid-like fluorescence, region IV (Ex: 250–400 nm–Em: 290–380 nm) related to soluble microbial byproduct-like (SMP-like) fluorescence, and region V (Ex: 250–400 nm–Em: 380–550 nm) assigned to humic acid-like fluorescence [33,34]. Chen et al. [5] proposed that integration beneath EEMs within selected regions represents the cumulative fluorescence response of DOM with similar properties. Important parameters in FRI were: (a) normalized region-specific EEM volume ($\Phi_{i,n}$), obtained by normalizing the volume beneath region "*i*" of the EEM to the fractional projected excitation-emission area and (b) cumulative EEM volume ($\Phi_{T,n}$), equal to the sum of $\Phi_{I,n}$–$\Phi_{V,n}$.

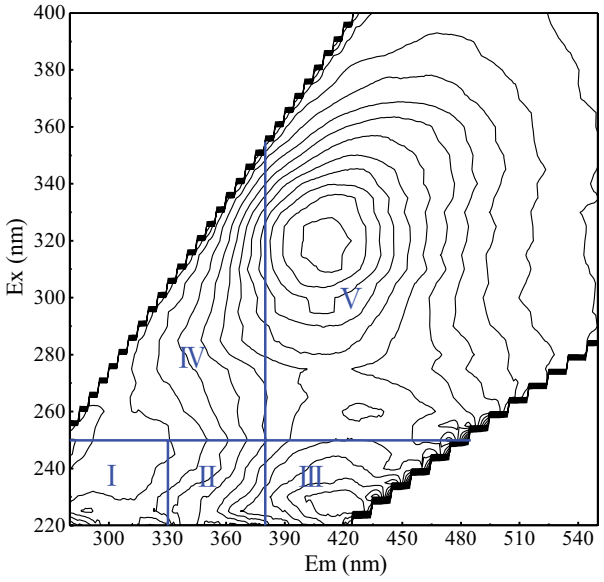


Fig. 4. Fluorescence spectra for the blank sample in the photodegradation experiments.

As shown in Figs. 4 and 5, photodegradation had caused dramatic changes in fluorescence characteristics of TPI-A in ice. Photodegradation resulted in increases of $\Phi_{I,n}$ and decreases of $\Phi_{II,n}$, $\Phi_{III,n}$, $\Phi_{IV,n}$ and $\Phi_{V,n}$ (Fig. 6), which indicated that in the photodegradation process of TPI-A in ice, aromatic protein-like II, fulvic acid-like, SMP-like, and humic acid-like fluorescent materials were removed and aromatic protein-like I fluorescent materials were produced. For $\Phi_{i,n}$ and $\Phi_{T,n}$, the difference value between blank and effect factors samples in each group was a reflection of the reduction of fluorescent materials due to photodegradation while the difference value between the maximum value and minimum value within a group reflected the influence of the factor examined in this group on the photodegradation of fluorescent materials. As shown in Fig. 6, the reduction of total fluorescent materials resulted from photodegradation was approximately 18.0%, while the differences in photodegradation rates of total fluorescent materials caused by pH, salinity, Fe concentration, $NO_3^-$ concentration, and original DOC concentration were 2.6%–12.5%. Thus it could be concluded that these factors had an unimportant influence on the photodegradation of the fluorescent materials in TPI-A in ice.

The maximum difference value of $\Phi_{T,n}$ removal rate resulted in pH variation was 12.5% (Fig. 6). Its influence ability on the total fluorescent substance removal rate was higher than other factors. When pH = 5.0, both $\Phi_{i,n}$ and $\Phi_{T,n}$ reached their peaks, which indicated such condition was unfavorable for the photodegradation of fluorescent materials in TPI-A in ice. In addition, the minimum value of $\Phi_{i,n}$ and $\Phi_{T,n}$ appeared in the sample of pH = 11.0, suggesting that in the photodegradation process, the alkaline condition was better for fluorescent materials removal in TPI-A than acidic condition.

The maximum difference value of $\Phi_{T,n}$ removal rate resulted from salinity variation was 11.1%. With increases of salinity, $\Phi_{I,n}$, $\Phi_{II,n}$, $\Phi_{III,n}$, and $\Phi_{IV,n}$ value increased while the $\Phi_{V,n}$ value was barely changed. Thus, it could be concluded from the results that high salinity inhibited the photodegradation of aromatic protein-like, fulvic acid-like, and SMP-like fluorescent materials in TPI-A while having no effect on the photodegradation of humic acid-like fluorescent materials.

As shown in Fig. 6, the maximum difference value of $\Phi_{T,n}$ removal rate resulted by Fe concentration variation was 2.6% which made Fe concentration the least influential factor of the five factors that influence the photodegradation of the total fluorescent materials. In comparison with other fluorescent materials, the photodegradation of aromatic protein-like I fluorescent materials seemed to be affected more by Fe concentration.

The maximum difference value of $\Phi_{T,n}$ removal rate resulted in $NO_3^-$ concentration variation was 7.9%. As indicated in Fig. 6, in the photodegradation process of TPI-A in the ice, $NO_3^-$ inhibited the photodegradation of five types of fluorescent materials and $NO_3^-$ had a greater influence on photodegradation of aromatic protein-like I and SMP-like fluorescent materials while its influence on photodegradation of humic acid-like fluorescent materials was negligible.

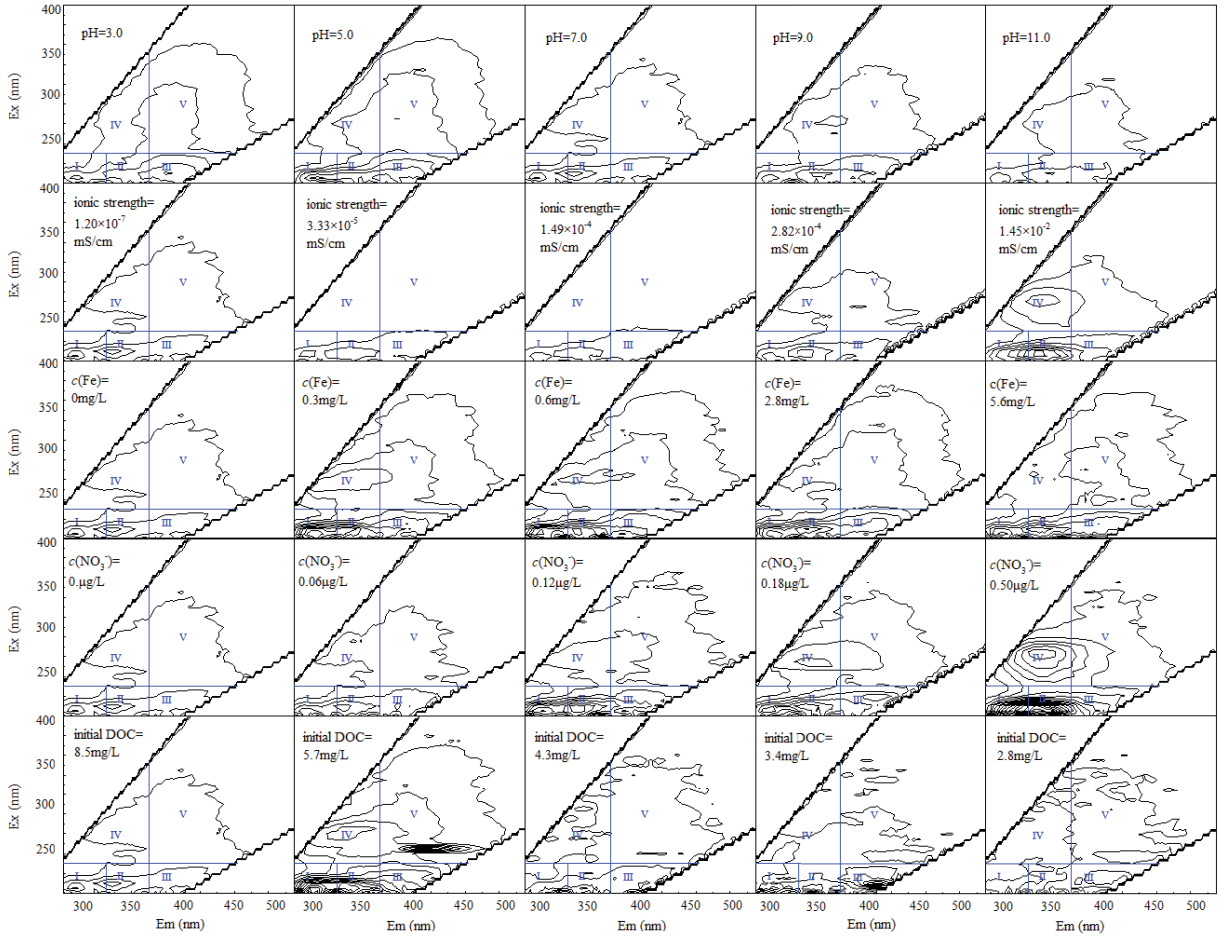


Fig. 5. Fluorescence spectra for samples in the photodegradation experiments.

The maximum difference value of $\Phi_{T,n}$ removal rate resulted from initial DOC concentration variation was 142.8%. With initial DOC concentration decreased from 8.5 to 2.8 mg $L^{-1}$ as well as the $\Phi_{T,n}$ removal rate decreased from 18.0% to –124.8%, it could be seen that in the photodegradation process of TPI-A in ice, lower initial DOC concentration resulted in the production of fluorescent materials.

### 3.4. THMFP and specific trihalomethane formation potential

THMFP is often the term employed to indicate the amount of THMs that could be produced during the chlorination process, and could indirectly represent the amount of THM precursors in water samples [35,36]. As shown in Fig. 7, the THMFP removal rate resulted from solar irradiation was 74.7%. The maximum differences in THMFP removal rates caused by variations of pH, salinity, Fe concentration, $NO_3^-$ concentration, and original DOC concentration were 15.2%, 56.5%, 10.2%, 13.1%, and 12.2%, indicating that salinity had a significantly greater influence on photodegradation of THM precursors in TPI-A in ice than the other factors.

In the photodegradation process of TPI-A in ice, comparing with pH = 7.0, both increases and decreases of pH could reduce the amount of THMFP (Fig. 7). Especially the increase of pH was very benefit for THMFP removal. Thus, it could be seen that high pH conditions effectively accelerated the photodegradation of THM precursors in TPI-A in ice.

In the photodegradation process of TPI-A in ice, when salinity was 0, the removal rate of THMFP was 74.7%; when salinity was 1~30, the removal rate of THMFP was 18.3%–51.7% (Fig. 7). Thus, it could be concluded from the results that the presence of inorganic salts inhibited the photodegradation of THM precursors and the higher the salinity was, the photodegradation rate of THM precursors was.

As shown in Fig. 7, THMFP of samples with Fe concentration of 0.3–2.8 mg $L^{-1}$ were higher than that with Fe concentration of 0 mg $L^{-1}$, which suggested that Fe concentration within such range inhibited the photodegradation of THM precursors. On the other hand, a higher Fe concentration of 5.6 mg $L^{-1}$ accelerated the photodegradation of THM precursors.

In the photodegradation process of TPI-A in ice, THMFP of the sample with $NO_3^-$ concentration of 0 was 50.4 μg $L^{-1}$ (Fig. 7). When $NO_3^-$ concentration was 0.06–0.50 mg $L^{-1}$, THMFP of the samples was 60.4–76.6 μg $L^{-1}$. The results suggested that the presence of $NO_3^-$ inhibited the photodegradation of

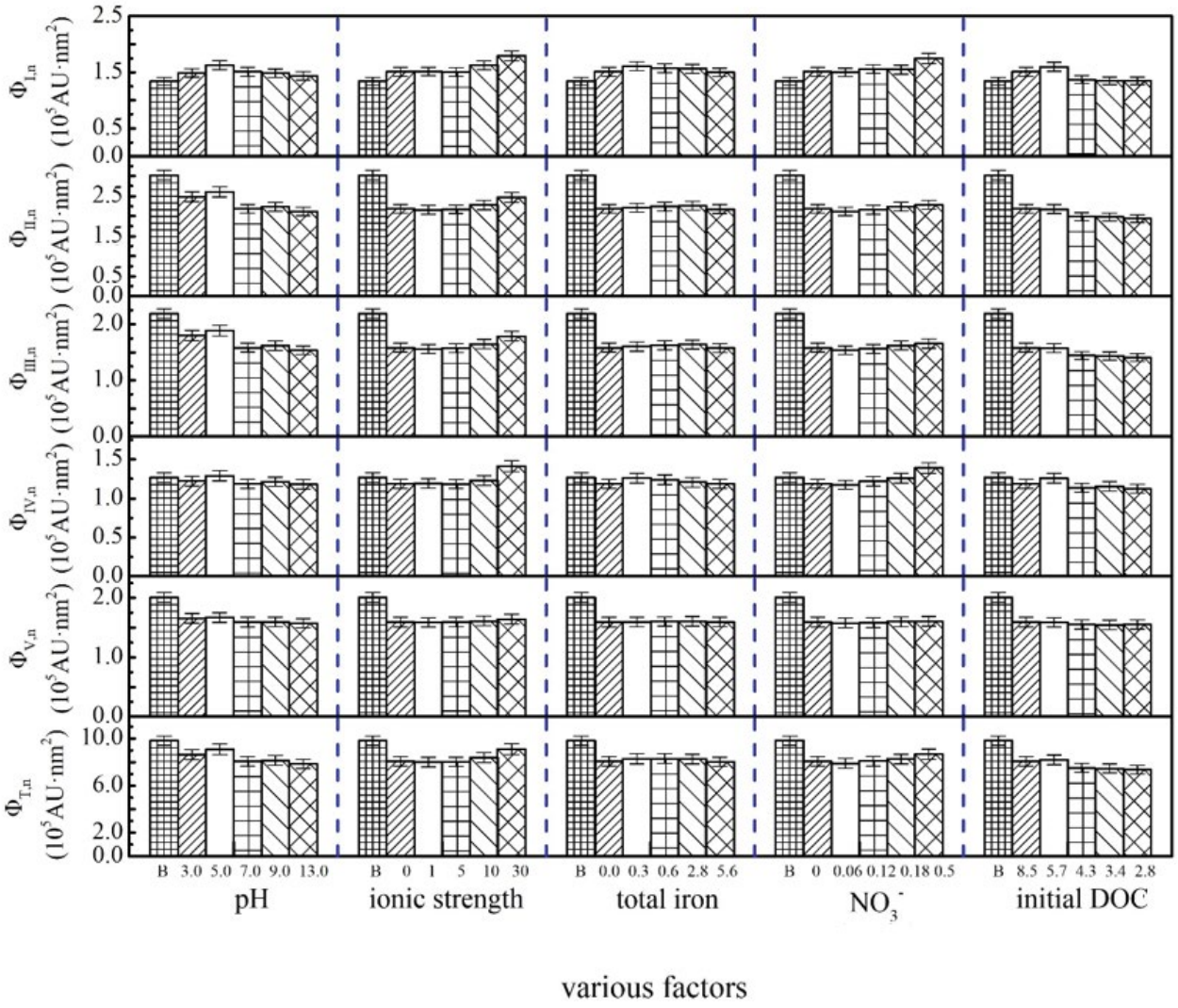


Fig. 6. (a) $\Phi_{I,n}$, (b) $\Phi_{II,n}$, (c) $\Phi_{III,n}$, (d) $\Phi_{IV,n}$, (e) $\Phi_{V,n}$, and (f) $\Phi_{T,n}$ values for samples in the photodegradation experiments.

THM precursors. When $NO_3^-$ concentration was 0.18 mg $L^{-1}$, the inhibition effect reached its peak.

As shown in Fig. 7, THMFP decreased with decreasing initial DOC, and the minimum THMFP observed in the sample with an initial DOC of 2.8 mg $L^{-1}$. When initial DOC concentration of samples decreased from 8.5 to 2.8 mg $L^{-1}$, the THMFP removal rates increased from 80.2% to 84.6%, indicating that the lower the initial DOC concentration was, the higher the removal rate of THM precursors was.

Because THMFP is dependent upon DOC concentration, the reactivity of DOC is also reported in terms of specific trihalomethane formation potential (STHMFP), that is, micrograms of THMFP formed per milligram of DOC precursor material in the water (μg $mg^{-1}$).

The STHMFP of samples in photodegradation experiments were shown in Fig. 8. In the photodegradation process, comparing with pH = 7.0, both increases of pH and decrease of pH resulted in a decrease of STHMFP of TPI-A, that is, the removal rates of THM precursors were greater than those of the bulk organics represented by DOC and the greater the pH increase or decrease was, the more obvious the effect was. Especially the high pH condition was beneficial for the photodegradation of THM precursors. The STHMFP of the sample with a pH of 11.0 was just half of that with a pH of 7.0.

In the photodegradation process of TPI-A in ice, THMFP increased with the increase of salinity while DOC decreased with the increase of salinity when salinity was lower than 5 (Figs. 1 and 7). As a result, STHMFP increased with the increase of salinity when salinity was lower than 5. When salinity was high than 5, a further increase of salinity had negligible influence over STHMFP.

When Fe concentration was lower than 0.6 mg $L^{-1}$, the increase of Fe concentration was more beneficial for the photodegradation of non-THM precursors and led to increases in STHMFP of TPI-A (Fig. 8). When Fe concentration was higher than 0.6 mg $L^{-1}$, the increase of Fe concentration was more beneficial for the photodegradation of THM precursors and resulted in decreases in STHMFP of TPI-A.

The influence of $NO_3^-$ over STHMFP was similar to that of Fe. With the increase of $NO_3^-$ concentration, the STHMFP of TPI-A gradually increased. When $NO_3^-$ concentration was

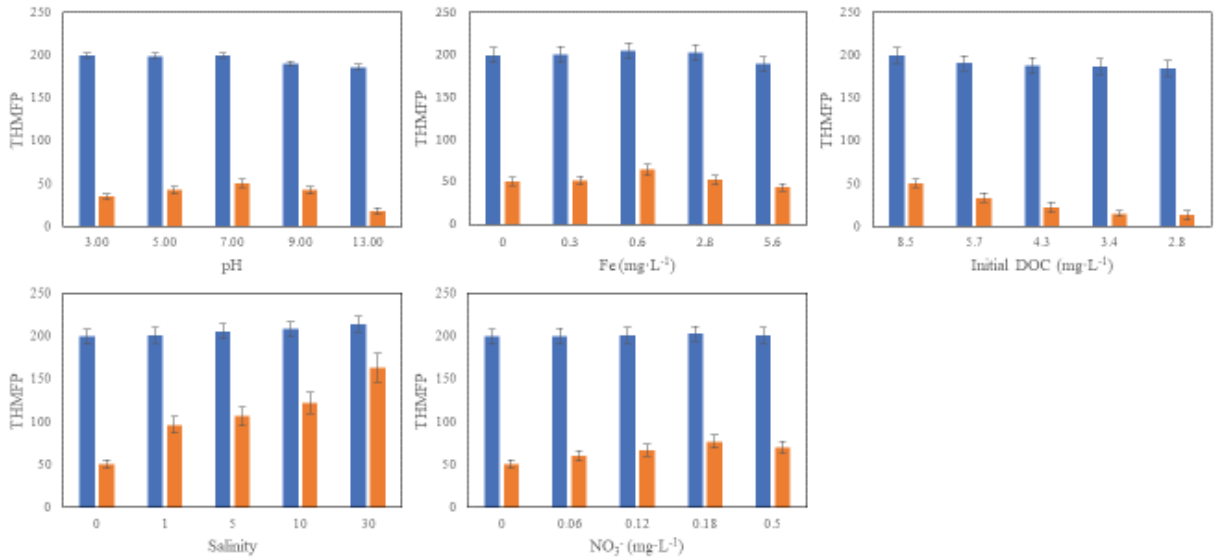


Fig. 7. THMFP for samples (a) with different pH, (b) with different Fe concentrations, (c) with different salinity values, (d) with different $NO_3^-$ concentrations, and (e) with different initial DOC values before and after photolysis 3 h.

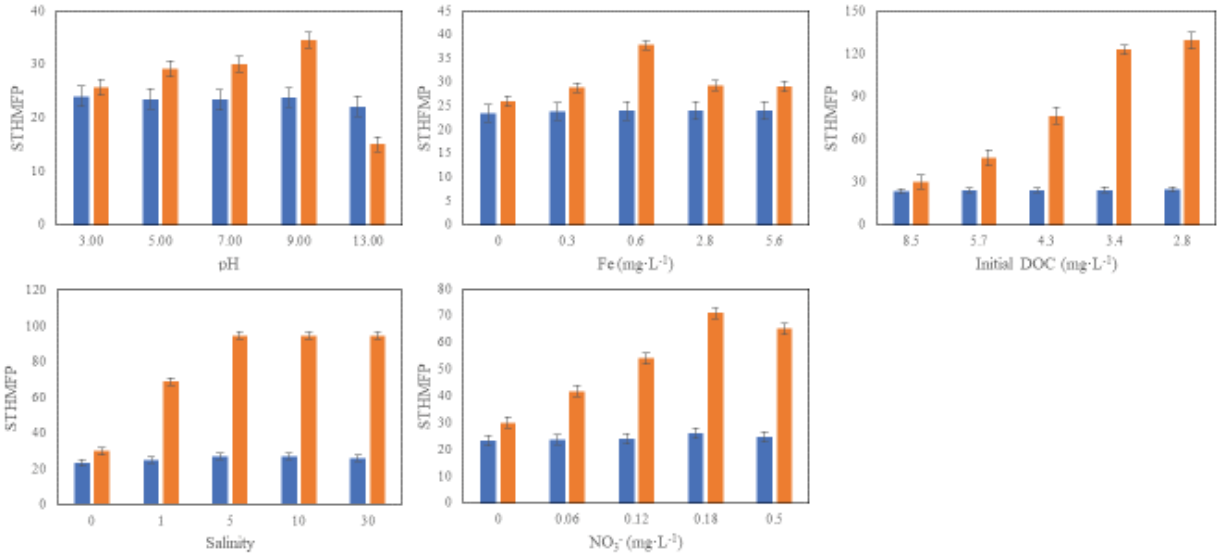


Fig. 8. STHMFP for samples (a) with different pH, (b) with different Fe concentrations, (c) with different salinity values, (d) with different $NO_3^-$ concentrations, and (e) with different initial DOC values before and after photolysis 3 h.

0.18 mg $L^{-1}$, the STHMFP value reached its peak. Further increase in $NO_3^-$ concentration resulted in the higher removal rate of THM precursors as compared with that of the bulk organics represented by DOC in the photodegradation process of TPI-A in ice.

The influence of initial DOC concentration over STHMFP of TPI-A was remarkable, in the photodegradation process of TPI-A in ice (Fig. 8). With the decrease of initial DOC concentration, the STHMFP gradually increased. Although the removal rates of both DOC and THMFP increased with decreasing initial DOC concentration as described earlier, the increasing degree of DOC removal rate was higher than that of THMFP, which resulted in the increased STHMFP of TPI-A after photodegradation.

## 4. Conclusions

The goal of this study was to investigate the effect of pH, salinity, the concentrations of Fe and $NO_3^-$, and original DOC concentration, on the photodegradation of TPI-A in ice under natural solar radiation. The following conclusions are drawn based on the experimental results:

- In the photodegradation process of TPI-A in the ice, compared with neutral conditions, both acidic and alkaline conditions accelerated DOC and UV-254 removal rates. High pH conditions effectively accelerated the photodegradation of fluorescent materials and THM precursors in TPI-A.

- Salinity inhibited the photodegradation of UV-absorbing compounds, THM precursors, and aromatic protein-like, fulvic acid-like, and soluble microbial byproduct-like (SMP-like) fluorescent materials in TPI-A.
- Influences of Fe concentration over the photodegradation of TPI-A and total fluorescent materials in it were small.
- $NO_3^-$ accelerated the photodegradation of TPI-A while it had an inhibition effect over five types of fluorescent materials in TPI-A.
- Lower the initial DOC concentration was, the higher the photodegradation rates TPI-A and THM precursors in it.

## Acknowledgments

The work was supported by the National Natural Science Foundation of China (No. 41771503), the China Scholarship Council Project (No.201906800009), the Innovative Team Project of Education Department of Liaoning Province (LT2018018) of China.

## References

[1] K.M. Parker, J.J. Pignatello, W.A. Mitch, Influence of ionic strength on triplet-state natural organic matter loss by energy transfer and electron transfer pathways, Environ. Sci. Technol., 47 (2013) 10987–10994.
[2] S. Bahnmüller, U. von Gunten, S. Canonica, Sunlight-induced transformation of sulfadiazine and sulfamethoxazole in surface waters and wastewater effluents, Water Res., 57 (2014) 183–192.
[3] S.I. Carvalho, M. Otero, A.C. Duarte, E.B. Santos, Spectroscopic changes on fulvic acids from a kraft pulp mill effluent caused by sun irradiation, Chemosphere, 73 (2008) 1845–1852.
[4] J. Chen, B. Gu, E.J. Le Boeuf, H. Pan, S. Dai, Spectroscopic characterization of the structural and functional properties of natural organic matter fractions, Chemosphere, 48 (2002) 59–68.
[5] W. Chen, P. Westerhoff, J.A. Leenheer, K. Booksh, Fluorescence excitation-emission matrix regional integration to quantify spectra for dissolved organic matter, Environ. Sci. Technol., 37 (2003) 5701–5710.
[6] A.T. Chow, F. Guo, S. Gao, R.S. Breuer, Size and XAD fractionations of trihalomethane precursors from soils, Chemosphere, 62 (2006) 1636–1646.
[7] G.L. Aiken, D.M. McKnight, K.A. Thorn, E.M. Thurman, Isolation of hydrophilic organic acids from water using nonionic macroporous resins, Org. Geochem., 18 (1992) 567–573.
[8] S. Xue, Q.L. Zhao, L.L. Wei, T. Jia, Trihalomethane formation potential of organic fractions in secondary effluent, J. Environ. Sci., 20 (2008) 520–527.
[9] D.M. Quanrud, M.M. Karpiscak, K.E. Lansey, R.G. Arnold, Transformation of effluent organic matter during subsurface wetland treatment in the Sonoran Desert, Chemosphere, 54 (2004) 777–788.
[10] S. Xue, Q.L. Zhao, L.L. Wei, N.Q. Ren, Behavior and characteristics of dissolved organic matter during column studies of soil aquifer treatment, Water Res., 43 (2009) 499–507.
[11] B.A. Cottrell, M. Gonsior, S.A. Timko, A.J. Simpson, W.J. Cooper, W. van der Veer, Photochemistry of marine and fresh waters: a role for copper–dissolved organic matter ligands, Mar. Chem., 162 (2014) 77–88.
[12] Y. Du, H. Chen, Y. Zhang, Y. Chang, Photodegradation of gallic acid under UV irradiation: insights regarding the pH effect on direct photolysis and the ROS oxidation-sensitized process of DOM, Chemosphere, 99 (2014) 254–260.
[13] A. El-Ghenymy, R.M. Rodríguez, C. Arias, F. Centellas, J.A. Garrido, P.L. Cabot, E. Brillas, Electro-Fenton and photoelectro-Fenton degradation of the antimicrobial sulfamethazine using a boron-doped diamond anode and an air-diffusion cathode, J. Electroanal. Chem., 701 (2013) 7–13.
[14] J.B. Fellman, K. Petrone, P. Grierson, Leaf litter age, chemical quality, and photodegradation control the fate of leachate dissolved organic matter in a dryland river, J. Arid Environ., 89 (2013) 30–37.
[15] W. Feng, D. Nansheng, Photochemistry of hydrolytic iron (III) species and photoinduced degradation of organic compounds. A mini review, Chemosphere, 41 (2000) 1137–1147.
[16] M.T. Ghaneian, P. Morovati, M.H. Ehrampoush, M. Tabatabaee, Humic acid degradation by the synthesized flower-like Ag/ZnO nanostructure as an efficient photocatalyst, J. Environ. Health Sci. Eng., 12 (2014) 138.
[17] C.L. Kang, X.J. Tang, P. Guo, H.J. Gao, F. Peng, X.J. Liu, Photoconversion of phenol in ice with the presence of nitrate, Chem. J. Chinese U., 4 (2009) 757–761.
[18] V. Kavitha, K. Palanivelu, The role of ferrous ion in Fenton and photo-Fenton processes for the degradation of phenol, Chemosphere, 55 (2004) 1235–1243.
[19] H.C. Kim, M.J. Yu, Characterization of natural organic matter in conventional water treatment processes for selection of treatment processes focused on DBPs control, Water Res., 39 (2005) 4779–4789.
[20] H.C. Kim, M.J. Yu, I. Han, Multi-method study of the characteristic chemical nature of aquatic humic substances isolated from the Han River, Korea, Appl. Geochem., 21 (2006) 1226–1239.
[21] J. Klanova, P. Klan, J. Nosek, I. Holoubek, Environmental ice photochemistry: monochlorophenols, Environ. Sci. Technol., 37 (2003) 1568–1574.
[22] S. Xue, C. Wang, Z.H. Zhang, Y.T. Song, Q. Liu, Photodegradation of dissolved organic matter in ice under solar irradiation, Chemosphere, 144 (2016) 816–826.
[23] J.-P. Croueä, M.F. Benedetti, D. Violleau, J.A. Leenheer, Characterization and copper binding of humic and nonhumic organic matter isolated from the South Platte River: evidence for the presence of nitrogenous binding site, Environ. Sci. Technol., 37 (2003) 328–336.
[24] R.G. Zepp, B.C. Faust, J. Holgné, Hydroxyl radical formation in aqueous reactions (pH 3–8) of iron(II) with hydrogen peroxide: the photo-Fenton reaction, Environ. Sci. Technol., 26 (1992) 313–319.
[25] S. Lofts, E. Tipping, J. Hamilton-Taylor, The chemical speciation of Fe(III) in freshwaters, Aquat. Geochem., 14 (2008) 337–358.
[26] M.V. Shankar, S. Nélieu, L. Kerhoas, J. Einhorn, Photo-induced degradation of diuron in aqueous solution by nitrites and nitrates: kinetics and pathways, Chemosphere, 66 (2007) 767–774.
[27] J. Chen, S.O. Pehkonen, C.J. Lin, Degradation of monomethylmercury chloride by hydroxyl radicals in simulated natural waters, Water Res., 37 (2003) 2496–2504.
[28] S.A. Timko, M. Gonsior, W.J. Cooper, Influence of pH on fluorescent dissolved organic matter photo-degradation, Water Res., 85 (2015) 266–274.
[29] C.M. Glover, F.L. Rosario-Ortiz, Impact of halides on the photoproduction of reactive intermediates from organic matter, Environ. Sci. Technol., 47 (2013) 13949–13956.
[30] C. Liang, H. Zhao, M. Deng, X. Quan, S. Chen, H. Wang, Impact of dissolved organic matter on the photolysis of the ionizable antibiotic norfloxacin, J. Environ. Sci., 27 (2015) 115–123.
[31] S. Xue, Q.L. Zhao, X. Ma, F. Li, J. Wang, L.L. Wei, Comparison of dissolved organic matter fractions in a secondary effluent and a natural water, Environ. Monit. Assess., 180 (2011) 371–383.
[32] L. Zhou, Y. Zhang, Q. Wang, C. Ferronato, X. Yang, J.-M. Chovelon, Photochemical behavior of carbon nanotubes in natural waters: reactive oxygen species production and effects on •OH generation by Suwannee River fulvic acid, nitrate, and Fe(III), Environ. Sci. Pollut. Res., 23 (2016) 19520–19528.
[33] S. Xue, Q. Zhao, L. Wei, Y. Song, M. Tie, Fluorescence spectroscopic characterization of dissolved organic matter fractions in soils in soil aquifer treatment, Environ. Monit. Assess., 185 (2013) 4591–4603.

[34] X. Yang, F. Meng, G. Huang, L. Sun, Z. Lin, Sunlight-induced changes in chromophores and fluorophores of wastewater-derived organic matter in receiving waters–the role of salinity, Water Res., 62 (2014) 281–292.
[35] C. Zeri, Ş. Beşiktepe, A. Giannakourou, E. Krasakopoulou, M. Tzortziou, D. Tsoliakos, A. Pavlidou, G. Mousdis, E. Pitta, M. Scoullos, Chemical properties and fluorescence of DOM in relation to biodegradation in the interconnected Marmara–North Aegean Seas during August 2008, J. Mar. Syst., 135 (2014) 124–136.
[36] G. Zhu, J. Yin, P. Zhang, X. Wang, G. Fan, B. Hua, B. Ren, H. Zheng, B. Deng, DOM removal by flocculation process: fluorescence excitation–emission matrix spectroscopy (EEMs) characterization, Desalination, 346 (2014) 38–45.